Enforcing Local Power Conservation for Metasurface Design Using Electromagnetic Inversion

Trevor Brown[*], Yousef Vahabzadeh[†], Christophe Caloz[†], and Puyan Mojabi[*]

[*]Department of Electrical and Comp. Engineering, University of Manitoba, Winnipeg, Canada, umbrow47@myumanitoba.ca

[†]Department of Electrical Engineering, École Polytechnique de Montréal, Montréal, Canada, christophe.caloz@polymtl.ca

Abstract—A method based on electromagnetic inversion is extended to facilitate the design of passive, lossless, and reciprocal metasurfaces. More specifically, the inversion step is modified to ensure that the field transformation satisfies local power conservation, using available knowledge of the incident field. This paper formulates a novel cost functional to apply this additional constraint, and describes the optimization procedure used to find a solution that satisfies both the user-defined field specifications and local power conservation. Lastly, the method is demonstrated with a two-dimensional (2D) example.

Index Terms—Electromagnetic metasurfaces, inverse problems, inverse source problems, optimization, antenna design

I. INTRODUCTION

Over the past decade, metasurfaces have emerged as useful devices for controlling electromagnetic radiation [1]–[6]. These subwavelength thin metamaterials can support arbitrary field transformations in a systematic fashion by imposing appropriate surface boundary conditions, providing a level of control over some *desired* field produced by a known *incident* field. This fundamental ability has led to a variety of applications, including generalized refraction and reflection [7], polarization manipulation [8], [9], spatial processing [10], and others.

In order to design a metasurface to support a field transformation, the tangential electric and magnetic fields must be known on either side of the boundary imposed by the metasurface. Most existing design procedures are limited to problems in which the output field is known analytically on the output side of the metasurface, which is satisfactory for well-defined problems such as plane wave refraction [11]. We recently developed a design method which facilitates output field specifications in a less restrictive manner [12]. Using this method, the field specifications can be at arbitrary locations external to the metasurface, either with or without phase information. Furthermore, the desired field can also be specified as a set of *performance* criteria, such as main beam direction(s), null location(s), beamwidth, or polarization. While this method allows for more general field specifications, it does not take advantage of prior knowledge of the incident field and consequently requires loss and/or gain to support the resulting field transformation.

In this work, we extend the method presented in [12] to allow for the design of lossless, passive, and reciprocal metasurfaces. This method uses electromagnetic inversion to solve for a set of tangential output (transmitted) fields that produce some user-specified field. This work modifies the inversion process by incorporating an additional step that penalizes solutions that do not satisfy local power conservation (LPC) using the known information about the incident field. Once an appropriate solution is found that satisfies both the field specifications and LPC, surface susceptibilities can be computed to support the transformation.

In this paper, we begin by presenting a brief review of the design procedure without enforcing LPC in Section II. In Section III we discuss and derive the constraint used to enforce LPC, and Section IV describes how the inversion process is modified to account for this new constraint. A preliminary example is presented in Section V, followed by some conclusions and a discussion of possible extensions to this work.

II. INVERSE SOURCE DESIGN FRAMEWORK

Herein, we present a brief review of the design method presented in [12], in which the main goal is to find tangential fields on the *output* side of the metasurface that satisfy some set of user-defined field specifications S in some external region of interest (ROI). An overview of the problem is depicted in Figure 1. We denote the input and output surface boundaries of the metasurface as Σ^- and Σ^+, respectively. The tangential fields (denoted as such by the subscript t) that we require to design the metasurface consist of the total fields on Σ^-, $\vec{E}_t^-$ and $\vec{H}_t^-$ (consisting of the incident and reflected fields), and the transmitted fields on Σ^+, $\vec{E}_t^+$ and $\vec{H}_t^+$. The user-defined specifications S fall into three general categories, ordered from most to least specific (i.e., most to least information):

1) Complex (amplitude and phase) field distributions (either in the near-field or far-field regions)
2) Phaseless field distributions (i.e., amplitude-only, power pattern)
3) Far-field performance criteria (i.e., main beam directions(s), null locations, beamwidth, etc.)

First, an electromagnetic inverse source problem is solved to find a set of equivalent electric ($\vec{J}$) and magnetic ($\vec{M}$) currents that produce the field specifications in the ROI. The domain upon which the equivalent currents are reconstructed,
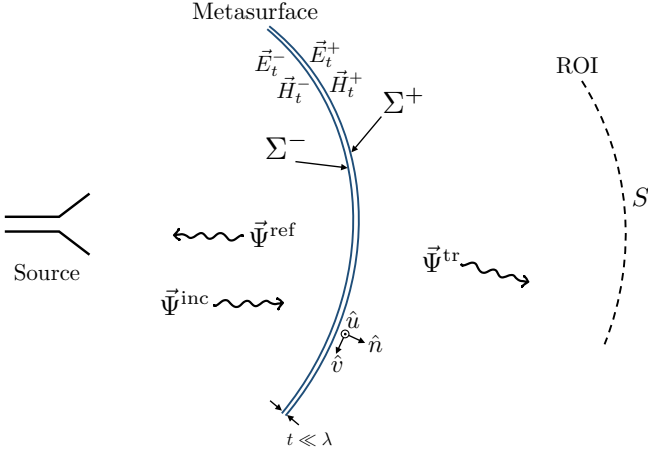
Fig. 1. Visual overview of the metasurface design problem. The internal and external surface boundaries of the metasurface are denoted by Σ^- and Σ^+, respectively. Some source generates an incident field $\vec{\Psi}^{\text{inc}}$ which interacts with the metasurface, producing both a reflected field $\vec{\Psi}^{\text{ref}}$ and a transmitted field $\vec{\Psi}^{\text{tr}}$. The tangential components of the electric and magnetic fields on Σ^- are denoted as $\vec{E}_t^-$ and $\vec{H}_t^-$, while the tangential fields on Σ^+ are denoted as $\vec{E}_t^+$ and $\vec{H}_t^+$. The user-defined field specifications S are defined on some of interest (ROI) external to the metasurface. Since the metasurface may be of arbitrary shape, we define the local coordinate system $(\hat{u}, \hat{v}, \hat{n})$ on Σ^+, where $\hat{n}$ is the unit outward normal to Σ^+. © 2019 IEEE. Reprinted, with permission, from [12] with minor modifications.

commonly referred to in inverse source problems as the 're-construction surface', is chosen to coincide with the physical boundary imposed by the metasurface. These currents are found by minimizing a cost functional, which we denote herein as $\mathcal{C}_1(\vec{J}, \vec{M})$, using the conjugate gradient method. This functional quantifies the difference between the fields generated by the equivalent currents and the field specifications, although the exact form depends on the category of field specifications listed above (for more details see (12), (13), and (20) in [12]).

If Love's equivalence condition is enforced (i.e., enforcing that the equivalent currents produce null fields on the input side of the metasurface), then the resulting equivalent currents will be related to the desired transmitted fields as

$$\vec{H}_t^+ = -\alpha \hat{n} \times \vec{J} \qquad \text{and} \qquad \vec{E}_t^+ = \alpha \hat{n} \times \vec{M}, \quad (1)$$

where α is a real-valued scaling parameter. Introducing α does not affect the characteristics of the *normalized* radiated field, but allows for some flexibility that will be utilized in Section III.

Once the desired tangential transmitted fields are known, the generalized sheet transition conditions (GSTCs) [13] can be utilized to determine a set of surface susceptibilities to support the discontinuity from the (known) incident field and (desired) reflected field [6]. Assuming a time-dependency of $e^{j\omega t}$ and free space on either side of the metasurface, the relationship

can be written as

$$\begin{pmatrix} -\Delta H_v \\ \Delta H_u \end{pmatrix} = j\omega\epsilon_0 \begin{pmatrix} \chi_{\text{ee}}^{uu} & \chi_{\text{ee}}^{uv} \\ \chi_{\text{ee}}^{vu} & \chi_{\text{ee}}^{vv} \end{pmatrix} \begin{pmatrix} E_{u,\text{av}} \\ E_{v,\text{av}} \end{pmatrix}$$
$$+ j\omega\sqrt{\epsilon_0\mu_0} \begin{pmatrix} \chi_{\text{em}}^{uu} & \chi_{\text{em}}^{uv} \\ \chi_{\text{em}}^{vu} & \chi_{\text{em}}^{vv} \end{pmatrix} \begin{pmatrix} H_{u,\text{av}} \\ H_{v,\text{av}} \end{pmatrix} \quad (2a)$$

$$\begin{pmatrix} -\Delta E_u \\ \Delta E_v \end{pmatrix} = j\omega\mu_0 \begin{pmatrix} \chi_{\text{mm}}^{vv} & \chi_{\text{mm}}^{vu} \\ \chi_{\text{mm}}^{uv} & \chi_{\text{mm}}^{uu} \end{pmatrix} \begin{pmatrix} H_{v,\text{av}} \\ H_{u,\text{av}} \end{pmatrix}$$
$$+ j\omega\sqrt{\epsilon_0\mu_0} \begin{pmatrix} \chi_{\text{me}}^{vv} & \chi_{\text{me}}^{vu} \\ \chi_{\text{me}}^{uv} & \chi_{\text{me}}^{uu} \end{pmatrix} \begin{pmatrix} E_{v,\text{av}} \\ E_{u,\text{av}} \end{pmatrix}, \quad (2b)$$

where ω is the angular frequency of the time harmonic fields, and ϵ_0 and μ_0 are the permittivity and permeability of free space.[1] The subscripts and superscripts u and v denote the tangential components of the local coordinate system of each unit cell defined by $\hat{u} \times \hat{v} = \hat{n}$ and $\hat{u} \perp \hat{v}$. The χ terms represent the electric/magnetic (first subscript) surface susceptibility components in the presence of an electric/magnetic (second subscript) field excitation [14]. The difference and average fields are defined as

$$\Delta\vec{\Psi} \triangleq \vec{\Psi}^{\text{tr}} - \left(\vec{\Psi}^{\text{inc}} + \vec{\Psi}^{\text{ref}} \right) \quad (3)$$

$$\vec{\Psi}_{\text{av}} \triangleq \frac{\vec{\Psi}^{\text{tr}}|_{\Sigma^+} + \left(\vec{\Psi}^{\text{inc}}|_{\Sigma^-} + \vec{\Psi}^{\text{ref}}|_{\Sigma^-} \right)}{2}. \quad (4)$$

The final step in the design procedure is solving (2) for the non-zero susceptibility terms (depending on the problem, some χ terms may be assumed to be zero).

III. ENFORCING LOCAL POWER CONSERVATION

The main limitation of the procedure presented in Section II and [12] is that the synthesized susceptibilities may require (undesirable) loss and/or gain. To overcome this limitation, we first note that a necessary condition for a passive and lossless metasurface is that the input and output fields must satisfy LPC [15], [16]. That is, the real power incident on each unit cell must be equal to the real power transmitted from each unit cell, as indicated by the following equation that must hold along the metasurface:

$$\frac{1}{2} \text{Re}(\vec{E}_t^- \times \vec{H}_t^{-*}) = \frac{1}{2} \text{Re}(\vec{E}_t^+ \times \vec{H}_t^{+*}). \quad (5)$$

From this point onwards, we will assume 2D TE_z polarized fields and a 1D metasurface along the line $x = 0$ (i.e., $\hat{u} = \hat{z}$, $\hat{v} = \hat{y}$, and $\hat{n} = \hat{x}$) for notational simplicity, although the formulation would still hold for arbitrarily-shaped metasurfaces and 3D fields. We denote the left hand side of (5) evaluated at the ith unit cell as

$$p_i = \frac{1}{2} \text{Re}(E_y^- \times H_z^{-*})\Big|_{\text{unit cell } i}. \quad (6)$$

[1] The formulation shown here assumes that the normal components of the polarization densities are zero, both for mathematical convenience and since the tangential components are enough to uniquely define the fields.

Using (6) and the relationship between the equivalent currents and the tangential transmitted fields in (1), we can write the LPC constraint in (5) compactly as

$$\mathbf{p} = \frac{\alpha^2}{2} \operatorname{Re}(\mathbf{M} \odot \mathbf{J}^*) \tag{7}$$

where $\mathbf{J}$ and $\mathbf{M}$ are discretized vectors of the equivalent currents J_y and M_z at each unit cell, $\odot$ represents the element-wise Hadamard product, and $\mathbf{p}$ is a discrete vector of the real incident power calculated at each unit cell, with the ith element of $\mathbf{p}$ equal to p_i.

Separating the equivalent currents into their real and imaginary parts, denoted by the subscripts R and I, we have

$$
\begin{aligned}
\mathbf{p} &= \frac{\alpha^2}{2} \operatorname{Re}\left\{ (\mathbf{M}_R + j\mathbf{M}_I) \odot (\mathbf{J}_R - j\mathbf{J}_I) \right\} \\
&= \frac{\alpha^2}{2} (\mathbf{J}_R \odot \mathbf{M}_R + \mathbf{J}_I \odot \mathbf{M}_I).
\end{aligned}
\tag{8}
$$

At this point the restriction imposed by the LPC constraint becomes immediately obvious. Previously the equivalent currents had four degrees of freedom (i.e. $\mathbf{J}_R$, $\mathbf{J}_I$, $\mathbf{M}_R$, and $\mathbf{M}_I$) with which to satisfy the field specifications, but as shown in (8), the LPC constraint reduces the degrees of freedom to three. In other words, enforcing LPC results in a reduction in the dimension of the solution space, and may exclude some solutions that would have otherwise have satisfied the field constraints in an optimal manner.

We can now formulate a cost function to quantify the LPC constraint and include it in the design procedure. This term is formulated using (8) as

$$\mathcal{C}_2(\mathbf{J}, \mathbf{M}) = \kappa \frac{\left\| \mathbf{J}_R \odot \mathbf{M}_R + \mathbf{J}_I \odot \mathbf{M}_I - \frac{2}{\alpha^2} \cdot \mathbf{p} \right\|_2^2}{\left\| \frac{2}{\alpha^2} \cdot \mathbf{p} \right\|_2^2} \tag{9}$$

where $\| \cdot \|_2$ represents an L_2 norm and κ is a real-valued scalar weighting parameter used to balance the contribution of $\mathcal{C}_2$ during the optimization process discussed in the following section. Since we have complete freedom in selecting the scaling parameter α, it should be chosen in a way to minimize (9) for a given set of currents. Therefore, anytime (9) is evaluated, the α that results in the minimum of (9) is used.

IV. METHODOLOGY

Our unknowns consist of the separated real and imaginary parts of the electric and magnetic equivalent currents, which collectively we write for convenience as

$$\mathbf{x} = \begin{bmatrix} \mathbf{J}_R \\ \mathbf{J}_I \\ \mathbf{M}_R \\ \mathbf{M}_I \end{bmatrix} \tag{10}$$

First, $\mathcal{C}_1(\mathbf{x})$ is minimized *without* the LPC constraint using the conjugate gradient method as described in more detail in [12]. This provides an estimate for $\mathbf{x}$ that satisfies the field constraints and Love's condition prior to applying the LPC constraint. Next, particle swarm optimization is used to minimize

$$\mathcal{C}(\mathbf{x}) = \mathcal{C}_1(\mathbf{x}) + \mathcal{C}_2(\mathbf{x}), \tag{11}$$

with initial particle states set to the estimation for $\mathbf{x}$ obtained from the previous step. Once convergence is reached, the required tangential fields are obtained using (1).

Next, the susceptibility components required to support the desired transformation must be computed. As noted in [16], if we want to support a transformation of this nature without using loss and/or gain, we require more degrees of freedom than afforded by a monoisotropic metasurface. We overcome this limitation by allowing for the bianisotropic terms $\overline{\overline{\chi}}_{\mathrm{em}}$ and $\overline{\overline{\chi}}_{\mathrm{me}}$ (tensors collectively representing the various χ_{em} and χ_{me} terms in (2), respectively) to be non-zero, introducing magnetoelectric coupling to the metasurface.

Assuming 2D TE$_z$ fields with a 1D metasurface along $x = 0$, (2) simplifies to

$$-\Delta H_z = (j\omega\epsilon_0 E_{y,\mathrm{av}}) \chi_{\mathrm{ee}}^{yy} + (j\omega\sqrt{\mu_0\epsilon_0} H_{z,\mathrm{av}}) \chi_{\mathrm{em}}^{yz} \tag{12a}$$

$$-\Delta E_y = (j\omega\mu_0 H_{z,\mathrm{av}}) \chi_{\mathrm{mm}}^{zz} + (j\omega\sqrt{\mu_0\epsilon_0} E_{y,\mathrm{av}}) \chi_{\mathrm{me}}^{zy}. \tag{12b}$$

In order to avoid loss and gain, we first stipulate that χ_{ee}^{yy} and χ_{mm}^{zz} must be purely real [16]. Next, we note that if χ_{ee}^{yy} and χ_{mm}^{zz} are passive and lossless, the remaining condition for losslessness (i.e., $\overline{\overline{\chi}}_{\mathrm{em}}^T = \overline{\overline{\chi}}_{\mathrm{me}}^*$) must also hold since the field transformation satisfies LPC. If we enforce χ_{em}^{yz} and χ_{me}^{zy} to be purely imaginary, then any lossless and passive solution will also satisfy the condition of reciprocity (i.e., $\overline{\overline{\chi}}_{\mathrm{em}}^T = -\overline{\overline{\chi}}_{\mathrm{me}}$) [11]. This results in four real unknowns that must satisfy the two complex equations in (12), which can be directly computed assuming the tangential fields on both sides of the metasurface are known.

V. PRELIMINARY RESULTS

To illustrate the proposed method we attempt to design a reflectionless 1D metasurface to transform an incident TE$_z$ plane wave into a desired power pattern (phaseless field information only) specified in the far-field region. In this example, fields propagate in 2D in the xy plane, with the metasurface placed along the line $x = 0$. The frequency is 1 GHz and the metasurface unit cells are $\lambda/6$ in length, where λ represents the free space wavelength. The designed region of the metasurface exists from $y = -5\lambda$ to $y = 5\lambda$, with absorbing elements placed along the rest of the $x = 0$ line.

The incident field is a linearly tapered plane wave at normal incidence, with $|H_z| = 1$ A/m for $|y| \leq 7\lambda$ and linearly decreases to zero for $7\lambda < |y| \leq 10\lambda$. The desired phaseless power pattern is produced by simulating an array of 13 uniformly spaced $\hat{z}$-directed elementary dipoles along the y-axis between $y = -3\lambda$ and $y = 3\lambda$. The specified far-field power pattern is computed for $-90° \leq \varphi \leq 90°$ and shown in Figure 2.

The reconstruction surface upon which the equivalent currents are reconstructed is chosen to coincide with the metasurface, with the same $\lambda/6$ discretization. First, a solution is found by minimizing the cost functional *without* the LPC constraint. This solution is then used to initialize a particle swarm optimization algorithm that minimizes (11) using a
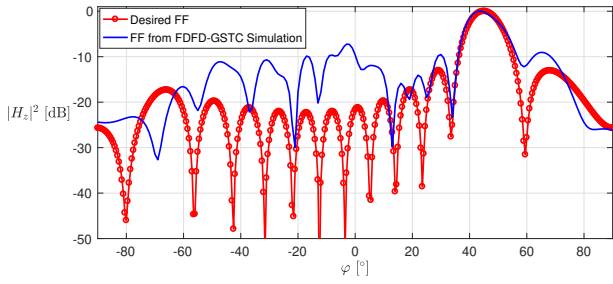
Fig. 2. Comparison of the (phaseless) far-field power pattern generated by the designed metasurface as simulated using the FDFD-GSTC solver (solid blue curve) and specified power pattern (solid red curve with circular markers).
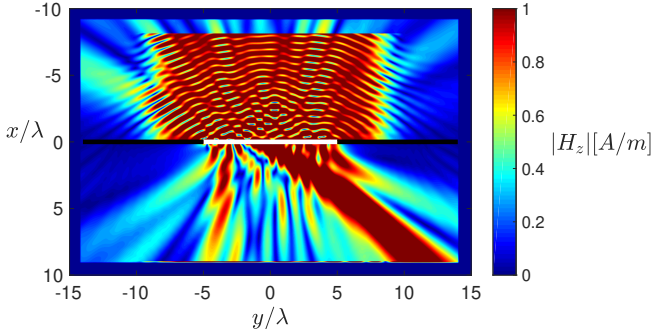

Fig. 3. Amplitude of H_z when the designed metasurface is illuminated by a normally incident linearly tapered plane wave, simulated using the FDFD-GSTC solver.

swarm size of 200 and a scaling factor of 0.02 for κ. The resulting solution is used to compute the four susceptibility terms using (1) and (12), which are necessarily passive, lossless, and reciprocal.

We then simulate the designed metasurface using a finite difference frequency domain (FDFD) GSTC solver, which modifies the standard FDFD formulation to impose the boundary conditions described by the GSTC equations [14]. The solution domain is $20\lambda \times 30\lambda$ in size and is bounded on all sides by a perfectly matched layer (PML) of thickness λ. The total magnetic field resulting from this simulation is shown in Figure 3, and the far-field pattern associated with this simulation is shown in Figure 2. These results show that the main features of the desired power pattern have been generated, although significant deviation in the specified side lobes does occur. The transmission efficiency, defined as the ratio of the real power transmitted through the metasurface to the real power incident on the metasurface, is 74.8%.

We speculate that the deviation from desired pattern is in part due to the non-zero reflection, clearly present in Figure 3. This unexpected reflection will be investigated and discussed at the conference along with additional examples.

VI. Conclusion

A metasurface design method was extended to ensure that the resulting field transformation satisfies local power conser-

vation, allowing for the design of passive, lossless, and reciprocal metasurfaces. A constraint on the equivalent currents was derived from the local power conservation relationship, and incorporated into the design procedure using a secondary optimization step. Non-zero magnetoelectric coupling terms are introduced to compensate for the loss of degrees of freedom resulting from excluding loss and gain. A preliminary 2D example was shown for the design of a passive, lossless, and reciprocal metasurface attempting to produce a specified (phaseless) power pattern, with relatively good agreement.

References

[1] C. L. Holloway, E. F. Kuester, J. A. Gordon, J. O'Hara, J. Booth, and D. R. Smith, "An overview of the theory and applications of metasurfaces: The two-dimensional equivalents of metamaterials," *IEEE Antennas and Propagation Magazine*, vol. 54, no. 2, pp. 10–35, 2012.

[2] C. Pfeiffer and A. Grbic, "Metamaterial Huygens' surfaces: Tailoring wave fronts with reflectionless sheets," *Phys. Rev. Lett.*, vol. 110, p. 197401, May 2013.

[3] M. Selvanayagam and G. Eleftheriades, "Discontinuous electromagnetic fields using orthogonal electric and magnetic currents for wavefront manipulation," *Optics Express*, pp. 14 409–14 429, 2013.

[4] S. Tretyakov, "Metasurfaces for general transformations of electromagnetic fields," *Philos. Trans. Royal Soc. A: Mathematical, Physical and Engineering Sciences*, vol. 373, no. 2049, p. 20140362, 2015.

[5] G. Minatti, M. Faenzi, E. Martini, F. Caminita, P. De Vita, D. Gonzlez-Ovejero, M. Sabbadini, and S. Maci, "Modulated metasurface antennas for space: Synthesis, analysis and realizations," *IEEE Transactions on Antennas and Propagation*, vol. 63, no. 4, pp. 1288–1300, April 2015.

[6] K. Achouri and C. Caloz, "Design, concepts and applications of electromagnetic metasurfaces," *Nanophotonics*, vol. 7, no. 6, pp. 1095–1116, 2018.

[7] V. S. Asadchy, M. Albooyeh, S. N. Tcvetkova, A. Díaz-Rubio, Y. Ra'di, and S. Tretyakov, "Perfect control of reflection and refraction using spatially dispersive metasurfaces," *Physical Review B*, vol. 94, no. 7, p. 075142, 2016.

[8] C. Pfeiffer and A. Grbic, "Bianisotropic metasurfaces for optimal polarization control: Analysis and synthesis," *Physical Review Applied*, vol. 2, no. 4, p. 044011, 2014.

[9] M. Selvanayagam and G. V. Eleftheriades, "Polarization control using tensor Huygens surfaces," *IEEE Transactions on Antennas and Propagation*, vol. 62, no. 12, pp. 6155–6168, 2014.

[10] K. Achouri, G. Lavigne, M. A. Salem, and C. Caloz, "Metasurface spatial processor for electromagnetic remote control," *IEEE Transactions on Antennas and Propagation*, vol. 64, no. 5, pp. 1759–1767, 2016.

[11] K. Achouri, M. A. Salem, and C. Caloz, "General metasurface synthesis based on susceptibility tensors," *IEEE Transactions on Antennas and Propagation*, vol. 63, no. 7, pp. 2977–2991, 2015.

[12] T. Brown, C. Narendra, Y. Vahabzadeh, C. Caloz, and P. Mojabi, "On the use of electromagnetic inversion for metasurface design," *IEEE Transactions on Antennas and Propagation*, pp. 1–13, 2019.

[13] M. M. Idemen, *Discontinuities in the electromagnetic field*. John Wiley & Sons (IEEE Press series on electromagnetic wave theory; 40), 2011.

[14] Y. Vahabzadeh, K. Achouri, and C. Caloz, "Simulation of metasurfaces in finite difference techniques," *IEEE Trans. Antennas Propag*, vol. 64, no. 11, pp. 4753–4759, 2016.

[15] A. Epstein and G. V. Eleftheriades, "Passive lossless Huygens metasurfaces for conversion of arbitrary source field to directive radiation," *IEEE Transactions on Antennas and Propagation*, vol. 62, no. 11, pp. 5680–5695, 2014.

[16] G. Lavigne, K. Achouri, V. S. Asadchy, S. A. Tretyakov, and C. Caloz, "Susceptibility derivation and experimental demonstration of refracting metasurfaces without spurious diffraction," *IEEE Transactions on Antennas and Propagation*, vol. 66, no. 3, pp. 1321–1330, 2018.